Mamey (*Mammea americana* L.) husks for the removal of Cr(VI) from aqueous media

J. Serrano-Gómez[a], C.S. Beltrán Vargas[b], J. Bonifacio-Martínez[a], M.T. Olguín[a],*

[a]*Instituto Nacional de Investigaciones Nucleares. Carretera México-Toluca S/N. La Marquesa, Ocoyoacac,
Edo. De México. C. P. 52750, Mexico, emails: teresa.olguin@inin.gob.mx (M.T. Olguín),
juan.serrano@inin.gob.mx (J. Serrano-Gómez), juan.bonifacio@inin.gob (J. Bonifacio-Martínez)*
[b]*Universidad Politécnica del Valle de Toluca. Carretera Toluca-Almoloya Km 56. Santiaguito Tlacilalcali,
Almoloya de Juárez. Edo. De México. C. P. 50904, Mexico, email: claris-1108@hotmail.com*

ABSTRACT

Mamey (*Mammea americana* L.) husks modified with formaldehyde (Mam-F) were used as adsorbents to remove Cr(VI) from aqueous solutions. Chromium adsorption was evaluated as a function of the initial pH, contact time, chromium concentration and temperature. The results showed that Cr(VI) was preferentially adsorbed by Mam-F at pH 2. Kinetics behavior was described by the pseudo-second-order model. According to Langmuir isotherm the maximum sorption capacity of Cr(VI) for Mam-F at pH 2 was 64.87 mg/g, higher than that observed at pH 6.5 (9.48 mg/g). Thermodynamic parameters revealed that chromium adsorption by Mam-F was an endothermic and non-spontaneous process.

Keywords: Cr(V) adsorption; Mamey husk; Formaldehyde-modification; Kinetic; Isotherms; Thermodynamics

1. Introduction

Due to the adverse toxicological effects of heavy metals released to aquatic systems from various industries and other sources, the environment is becoming increasingly polluted. Indeed, human beings are suffering the harmful effects of toxic metal pollutants, such as Cd, Pb, Cr, As, Hg, Cu and Ni. Among the aforementioned heavy metals, Cr is widely recognized as one of the most toxic elements, and its hexavalent compounds are carcinogenic and mutagenic [1]. In aquatic systems, chromium exists as trivalent Cr(III) and hexavalent Cr(VI), which is more toxic than Cr(III), even at low concentrations. Because Cr is used in many industries, such as battery manufacturing, metallurgical engineering, electroplating, mining and textile dying, the corresponding waste effluents contain Cr(VI) in concentrations that are well above the allowable limit of 0.05 mg/L, as defined by the United States Environmental Protection Agency.

Conventional methods for the removal of chromium from waste effluents to achieve the allowable limits before release into the environment include electrodialysis, solvent extraction, coagulation, ion exchange, chemical precipitation and adsorption. Adsorption processes have been widely used to separate heavy metals from aqueous solutions using different materials as adsorbents [2]. Thus, to obtain a low-cost and effective adsorption material for the removal of chromium from aqueous solutions, non-living materials obtained from plants have been investigated throughout the last decade. For instance, Garg et al. [3] studied the adsorption of Cr(VI) from aqueous solutions onto sugarcane bagasse, maize cobs and jatropha oil cake. The authors observed maximum adsorption in acidic media (pH 2) and a contact time of 60 min. In the aforementioned study, jatropha oil cake showed the highest adsorption capacity.

Furthermore, Sarin and Pant [4] assessed bagasse, eucalyptus bark, activated charcoal and charred rice for chromium removal and found that eucalyptus bark presented the highest Cr(VI) removal capacity, which was observed at pH 2.

* Corresponding author.

Potato peels, which are a low-cost agroindustry by-product, were used by Mutongo et al. [5] to search the removal of Cr(VI) from aqueous effluents. They found that an adsorbent dosage of 4 g/L was effective in complete removal of the metal ion, at pH 2.5, in 48 min. The adsorption data were fitted to the Langmuir isotherm, and a maximum monolayer adsorption capacity of 3.28 mg/g was calculated, suggesting a functional group limited adsorption process. Najim and Yassin [6] studied the utilization of modified pomegrenate peel shaken with distilled water (MPGP) and formaldehyde modified pomegrenate peel (FMPGP). The pH study showed that the optimal pH values of Cr(VI) removal by MPGP and FMPGP were 2.0 and 3.0, respectively. They also studied the effect of initial chromium concentration on the adsorption of Cr(VI) and determined maximum uptake capacities of 9.47 and 16.93 mg/g for MPGP and FMPGP, from Dubinin–Radushkevich (D–R) isotherm.

On the other hand, *Sargassum thunbergii* Kunste alga was evaluated [7] as adsorbent to remove Cr(VI) from aqueous solutions. The results showed that kinetics fitted the pseudo-second-order kinetic model and the thermodynamic parameters indicated and endothermic adsorption process. Also the equilibrium data followed well the Langmuir and Freundlich isotherm models, and the maximum adsorption capacity was 1.855 mmol/g at 318 K and pH 2.0. Pistachio hull was investigated by Moussavi and Barikbin [8] for the removal of hexavalent chromium from wastewater. Kinetic and isotherm modeling studies revealed that the experimental data best fit a pseudo-second-order and Langmuir model, respectively. The maximum Langmuir adsorption capacity was 116.3 mg/g. Wang et al. [9] used Alligator weed to investigate the removal of Cr(VI) from aqueous solutions. pH studies indicated that pH of 1.0 was most favorable for Cr(VI) removal. The kinetic data were analyzed using several models, and the results suggested that the Cr(VI) adsorption was best represented by the pseudo-second-order equation. Malkoc et al. [10] evaluated the waste pomace from an olive oil factory for the removal of Cr(VI) from aqueous solutions by performing batch and column experiments. According to their temperature studies, the thermodynamics of Cr(VI) adsorption onto pomace indicated the spontaneous and endothermic nature of the process. In column experiments, the total amount of adsorbed Cr(VI) and the adsorbed Cr(VI) content at equilibrium decreased with an increase in the flow rate but increased due to larger inlet chromium concentrations.

Palm branches were chemically modified [11] with an oxidizing agent (sulfuric acid) then coated with chitosan and surfactant (hexadecyltrimethylammonium bromide surfactant, HDTMA) to improve their Cr(VI) removal performance. It was found that Cr(VI) removal is pH dependent, and the maximum adsorption capacity obtained from the Langmuir model for the chitosan-coated oxidized palm branches was 55 mg/g. Other natural biomaterials such as *Ficus carica* bast fiber [12], *Tamarindus indica* [13], mosambi fruit peelings [14], *Ocimum americanum* L. seed pods [15], palm flower (*Borassus aethiopum*) [16], as well as activated neem leaves [17], activated carbon obtained from activated tamarind wood [18], boiled mamey husk [19] and activated tamarind seeds [20] have also been used as adsorbents for Cr(VI) removal from aqueous solutions. Thus, the aim of the present work was to

assess the performance of formaldehyde-modified mamey husk for the removal of Cr(VI) from aqueous media determining the effect of the pH, contact time, Cr(VI) concentration and temperature on Cr(VI) adsorption. The characterization of the formaldehyde-modified mamey husk was also considered in this work.

2. Materials and methods

2.1. Adsorbent

The raw mamey husks named as Mam were obtained from fruit bought in a local market in México City and were sun-dried for 2 weeks. The husks were crushed in an agate mortar and sieved to obtain particles with a mesh size of 25. Non-living *Mammea americana* L. biomass was repeatedly soaked in 0.2% aqueous formaldehyde until the solution was clear, which occurred after several treatments. The material was recovered by filtration and was allowed to dry at room temperature for 1 week. Thereafter, formaldehyde-modified mamey husks were referred to as Mam-F.

2.2. Cr(VI) solutions

The Cr(VI) adsorption experiments were performed using an aqueous solution containing 25 ppm of Cr (in the chemical form of CrO_4^{2-} ions) to simulate contaminated industrial effluents. The pH of the solution was 5.5.

2.3. Effect of pH

To determine the effect of pH on Cr(VI) adsorption, 0.100 g samples of Mam-F were agitated for 24 h in glass vials containing 10 mL of the 25 ppm Cr aqueous solution at different pH values, which ranged from 2 to 12, and a temperature of 20°C. After agitation, the suspension was centrifuged, and the liquid was recovered with a pipette. The solid was discarded, and the chromium content of the liquid was quantified using a Shimadzu UV–Vis spectrophotometer (model 265) at a wavelength of 372 nm. For each adsorption experiment, a chromium calibration curve was obtained using standard solutions of chromium in water.

2.4. Kinetics

The kinetics of the adsorption processes were determined under the experimental conditions described above. In all of the experiments, the initial pH was 5.5, and the agitation time of the suspensions was varied, ranging from 0.25 to 24 h. The adsorption data were fit to the pseudo-second-order kinetic model.

2.5. Adsorption isotherms

To obtain the adsorption isotherms, 100 mg of Mam-F were agitated as described above with 10 mL of either 50–500 ppm Cr solutions with a pH value of 6.5 or 500–1,000 ppm Cr solutions, whose pH was set to 2. Two experiments were carried out under the same conditions for each Cr concentration, and the chromium content of the recovered liquid was measured according to the aforementioned method. The

adsorption data were fit to the Freundlich, Langmuir and D–R model.

2.6. Thermodynamic

To understand the thermodynamic behavior of Cr(VI) adsorption by Mam-F, the assayed temperatures were 303, 313, 323 and 333 K, keeping constant the concentration (50 mg Cr/L) and contact time (24 h).

2.7. Characterization

2.7.1. Scanning electron microscopy

To obtain scanning electron microscopy images, samples of Mam-F before and after Cr adsorption were mounted directly onto the respective sample holder. The images were obtained at 25 keV using a Phillips XL30 electron microscope. Elemental analyses of the non-living biomass were performed via energy-dispersive X-ray electron spectroscopy using a DX-4 probe.

2.7.2. FT-IR Spectroscopy

The Fourier-Transform Infrared (FT-IR) spectra of Mam-F before and after contact with Cr solution were recorded in the 4,000–400 cm^{-1} range using a Nicolet Magna-IR 550 FT-IR. Analytical samples were prepared using the standard KBr pellet method.

2.7.3. pH of the point of zero charge (pH_{pzc})

The pH corresponding to the point of zero charge (pzc) for Mam-F was measured using the pH drift method [21–23]. Specifically, 0.15 g of Mam-F were combined with 50 mL of 0.01 M NaCl, and the initial pH was varied from 2 to 12. To adjust the pH, 0.1 M HCl and 0.1 M NaOH were added as needed to the solution. The suspensions were allowed to equilibrate for 48 h at 20°C, and the final pH values were determined using a pH STAT Controller (MeterLab PHM 290). The pH at which the corresponding curve intersected a straight line with a slope equal to 1 was considered the pH of the pzc.

3. Results and discussion

3.1. Effect of the initial pH

The effect of the initial pH on chromium adsorption is shown in Fig. 1, where the removal of Cr(VI) at equilibrium (%) is plotted against the initial pH. The maximum chromate ion removal was achieved at an initial pH of 2.0 and decreased with an increase in the initial pH. Thus, the optimum pH to adsorb Cr(VI) on Mam-F is 2. At pH 2 and a Cr content of 25 ppm, Cr(VI) ions were present in solute ion, primarily as $HCrO_4^-$ (~99%) and H_2CrO_4 (~1%), according to MEDUSA software [24]. As indicated by this computational program, at pH 4, $HCrO_4^-$ ions were the only species present in solution, while at pH 6 to 8, $HCrO_4^-$ and CrO_4^{2-} coexisted in variable ratios. At pH 10–12, only CrO_4^{2-} ions were present in solution. Thus, in acidic media, the chromium chemical species that adsorbed onto the positively charged active sites of Mam-F non-living biomass included $HCrO_4^-$ and CrO_4^{2-}. At low pH

values, active sites were abundant and primarily consisted of $-OH_2^+$ and $-NH_3^+$ groups, which formed when protons (H^+) became chemically bound to the $-OH$ and $-NH_2$ groups of the cellulose and hemicellulose in fiber and amino acids in proteins, respectively, both of which are organic components of mamey peels [25,26]. As a result, chromium anions were adsorbed by Mam-F due to the electrostatic attraction between $HCrO_4^-$ and CrO_4^{2-} anions and positively charged $-OH_2^+$ and $-NH_3^+$ groups. The proposed mechanism is supported by the fact that Cr(VI) adsorption increased at low pHs, while adsorption decreased when the pH was high [27] because the number of positive sites on Mam-F decreased.

3.2. Kinetics

The results of the kinetic of Cr(VI) adsorption on Mam-F are displayed in Fig. 2. Hexavalent chromium uptake by Mam-F was not fast, and a slow approach toward equilibrium was observed: saturation was achieved in approximately 17 h. The adsorption of Cr(VI) at equilibrium was 0.6491 mg/g, at an initial pH of 5.5.

To describe the Cr(VI) kinetic adsorption behavior by Mam-F, the experimental results were fitted to the pseudo-second-order and Elovich kinetic models. Both models have been considered for systems, which biomasses and heavy metals are involved [28,29].
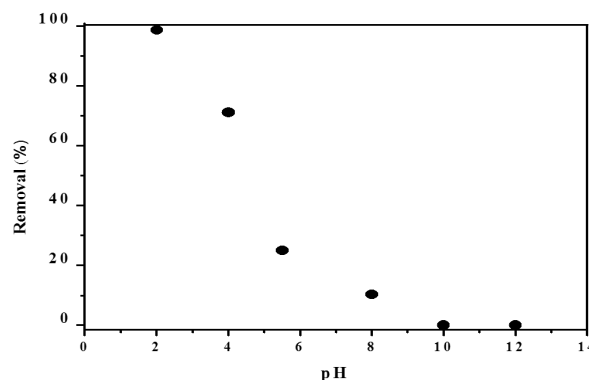
Fig. 1. Effect of pH on Cr(VI) adsorption by Mam-F.
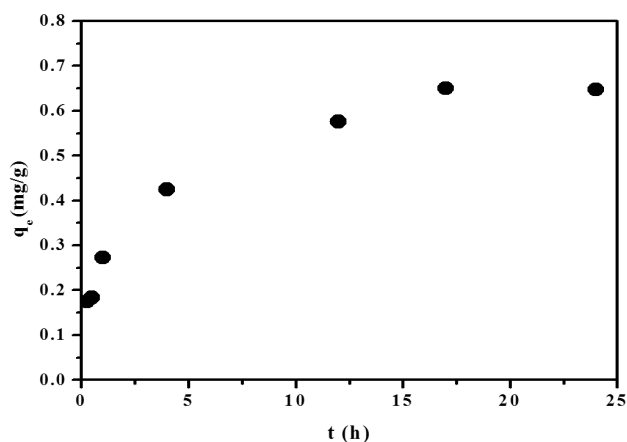
Fig. 2. Effect of contact time on the Cr(VI) adsorption by Mam-F at pH value of 5.5.

3.2.1. Pseudo-second-order model

This kinetic model [30] has been applied to heterogeneous systems, where the sorption mechanism is attributed to chemical sorption.

The pseudo-second-order rate equation can be expressed as follows:

$$\frac{t}{q_t} = \frac{1}{k_2 q_e^2} + \frac{1}{q_e} t \tag{1}$$

In Eq. (1), k_2 (g/mmol min) is the rate constant of the pseudo-second-order reaction, and q_t and q_e, which are given in units of mmol/g, are the amount of adsorbed Cr(VI) at a given time and the amount of adsorbed Cr(VI) at equilibrium, respectively. Fig. 3 presents a plot of t/q_t vs. t for the removal of Cr(VI) at an initial pH of 5.5. The linear relationship observed in this plot and the high value of the determination coefficient ($R^2 = 0.9919$) indicated that the Cr(VI) adsorption process obeyed pseudo-second-order kinetics. The initial adsorption rate (h) was given by the product $k_2 q_e^2$. In the present case, the values of q_e, k_2 and $k_2 q_e^2$ were 1.20×10^{-2} mmol/g, 1.167 g/mmol min, and 1.68×10^{-4} mmol/g min, respectively. The value of the calculated equilibrium adsorption data, q_e, was close to the experimental results (1.25×10^{-2} mmol/g). Thus, chemisorption played an important role in the removal of Cr(VI) by Mam-F.

3.2.2. Elovich model

The Elovich kinetic model is applied to chemisorption kinetic. The model indicates that the active sites are heterogeneous in nature and therefore exhibit different activation energies for chemisorption. The Elovich equation is based on the adsorption capacity of the adsorbent, and its linear form is as follows:

$$q_t = \frac{1}{\beta} \ln(\alpha\beta) + \frac{1}{\beta} \ln(t) \tag{2}$$
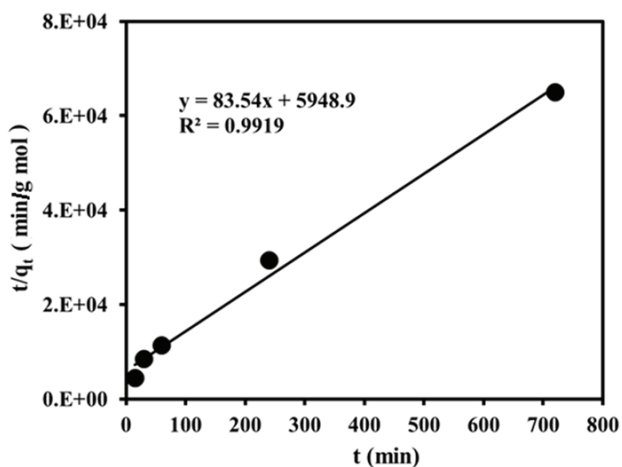
where q_t (mg/g min) is the metal uptake at time t; α is the initial adsorption rate (mg/g min) and β is the desorption constant (g/mg). The constant β and α are calculated from the slope and intercept of the straight line obtained when plotting q_t vs. $\ln(t)$ (Fig. 4). Thus, the values of these constants were found to be 9.26 g/mg and 0.0259 (mg/g min), with $R^2 = 0.9754$. High determination coefficients (R^2) for the pseudo-second-order and the Elovich kinetic models imply that the rate limiting is the chemical sorption.

It is important to note that the pseudo-second-order kinetic model describe better the Cr(VI) kinetic adsorption by Mam-F at pH 5.5 than the Elovich model. This result is in agreement with those reported in the literature using biosorbents to remove heavy metals from aqueous media [28,29].

3.3. Adsorption isotherms

The influence of chromium concentration on the adsorption of chromate ions by Mam-F was searched utilizing Cr(VI) solutions with concentrations ranging from 50 to 500 ppm. The pH values of these Cr(VI) aqueous solutions were around 6.5. On the other hand, when the effect of the initial pH was investigated, the optimum pH for Cr(VI) adsorption onto Mam-F was found to be 2. Thus, the influence of chromium concentration was also investigated by using Cr(VI) solutions with a pH value of 2, adjusted with HCl. Because of Cr(VI) sorption was very high at pH 2, the Cr concentrations utilized in this case varied from 500 to 1,000 ppm. The results showed that for both pH values, the percentage of adsorption decreased as the initial concentration of Cr(VI) increased because less active sites were available for adsorption, and a greater amount of sorbing species were present at higher chromium concentrations. Cr(VI) adsorption data were analyzed using Freundlich, Langmuir and D–R adsorption isotherms. In Fig. 5, the logarithm of the amount of chromium adsorbed per gram ($\log q_e$) of Mam-F is plotted against the logarithm of the chromium concentration in solution ($\log C_e$). q_e and C_e were determined at equilibrium, when the pH of the chromate solutions (500–1,000 ppm) was 2. A similar plot (Fig. 6) was obtained when the adsorption experiments were carried out using chromate solutions (50–500 ppm) with a

Fig. 3. Adsorption kinetics of Cr(VI) by Mam-F fitted to the pseudo-second-order model at pH value of 5.5.
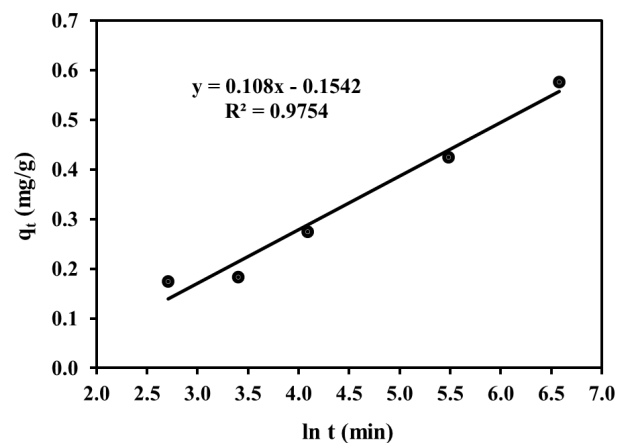
Fig. 4. Adsorption kinetics of Cr(VI) by Mam-F fitted to the Elovich model at pH value of 5.5.

pH of 6.5. The straight lines and high determination coefficients obtained in both cases clearly indicated that Cr(VI) adsorption on Mam-F could be described by the Freundlich isotherm in its logarithmic form (Eq. (3)):

$$\log q_e = \frac{1}{n} \log C_e + \log K_F \qquad (3)$$

where K_F and $1/n$ ($0 < 1/n < 1$) are the Freundlich constants. K_F [(mg/g) (L/mg)$^{1/n}$] is an indicator of the adsorption capacity of an adsorbent, while $1/n$ is related to the intensity of the adsorption process. The values of K_F and $1/n$ were computed using the least squares technique, yielding a value of 3.17×10^{-3} [(mol/g) (L/mol)$^{1/n}$] and 0.64 ($R^2 = 0.9977$) at pH 6.5. For pH 2, the corresponding values were 2.88×10^{-3} [(mol/g) (L/mol)$^{1/n}$] and 0.13 ($R^2 = 0.9963$). The adsorption intensity (n) for Cr(VI) was 1.56 and 7.69 at a pH of 6.5 and 2, respectively. These values were between 1 and 10, which indicated a favorable adsorption [31]. Because the values of $1/n$ in the present study were <1, the Freundlich isotherm was valid for Cr(VI) ion adsorption on Mam-F; thus, the adsorbent surface was heterogeneous, and the active centers showed an exponential distribution.

The Cr(VI) adsorption data for Mam-F were also fitted to the Langmuir isotherm. The Langmuir isotherm model is based on monolayer sorption onto a surface, which has a finite number of identical sites, and these sites are homogeneously distributed over the sorbent surface.

The Langmuir isotherm equation was expressed in the linearized form (Eq. (4)):

$$\frac{C_e}{q_e} = \frac{1}{K_L q_{max}} + \frac{C_e}{q_{max}} \qquad (4)$$

where K_L and q_{max} are the Langmuir constants and are related to the adsorption energy and maximum adsorption capacity, respectively. The linear plot shown in Fig. 7 was obtained when C_e/q_e was plotted vs. C_e for adsorption data obtained from chromium solutions (500–1,000 ppm) at pH 2.

A similar plot was also obtained when the pH of the chromium solution (50–500 ppm) was 6.5 (Fig. 8). The slope of the plot in Fig. 7 provided a maximum adsorption capacity
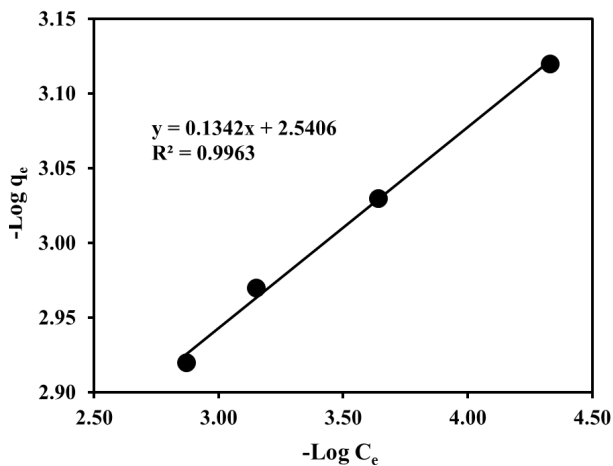
Fig. 5. Sorption isotherm of Cr(VI) by Mam-F at pH 2.0 fitted to the Freundlich model.
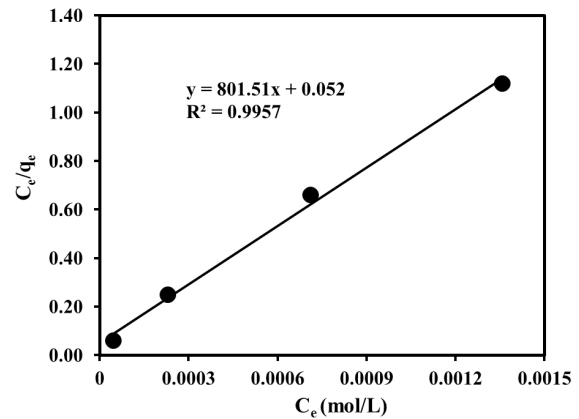
Fig. 7. Sorption isotherm of Cr(VI) by Mam-F at pH 2.0 fitted to the Langmuir model.
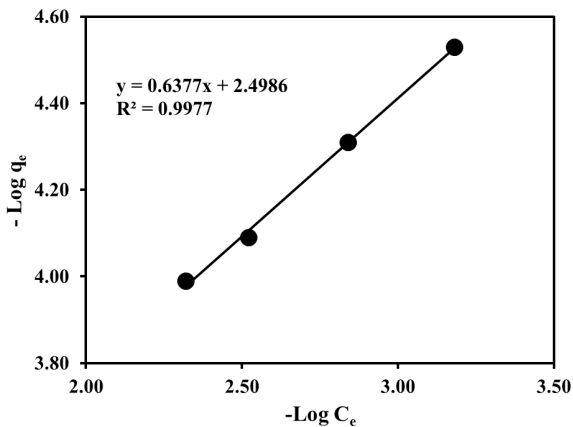
Fig. 6. Sorption isotherm of Cr(VI) by Mam-F at pH 6.5 fitted to the Freundlich model.
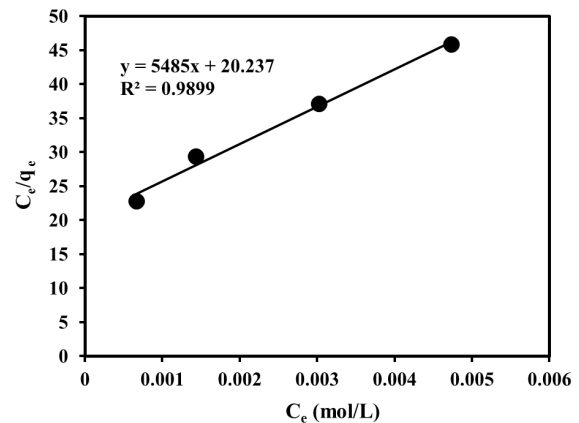
Fig. 8. Sorption isotherm of Cr(VI) by Mam-F at pH 6.5 fitted to the Langmuir model.

(q_{max}) of 64.87 mg/g for pH 2, while the intercept yielded a value of $K_L = 1.54 \times 10^4$ L/mol, and $R^2 = 0.9957$. Similarly, when the pH of the chromate solution was 6.5, the values of q_{max} and K_L were 9.48 mg/g and 271.06 L/mol, respectively, with $R^2 = 0.9899$ (Fig. 8). These results showed that q_{max} of Mam-F for Cr(VI) adsorption was ~6.8 times greater at pH 2 than at pH 6.5, and the value of R^2 was slightly higher.

The Cr(VI) adsorption data for Mam-F were also analyzed using the D–R isotherm model, which was expressed in its linearized form (Eq. (5)):

$$\ln q_e = \ln q_{max} - K_{D-R}\varepsilon^2 \tag{5}$$

The definition of q_e and q_{max} was described in a previous section; K_{D-R} is a constant related to the ion adsorption energy (mol^2 kJ^{-2}), and ε is the Polanyi potential (kJ mol^{-1}), which was calculated using the following Eq. (6):

$$\varepsilon = RT\ln\left(1 + \frac{1}{C_e}\right) \tag{6}$$

where R (8.314 J mol^{-1} K^{-1}) is the gas constant; T is the absolute temperature in degrees Kelvin; and C_e is the adsorbate equilibrium concentration (mg/L).

A straight line was obtained when $\ln q_e$ was plotted against ε^2, as shown in Figs. 9 and 10 for pH values of 2 and 6.5, respectively, indicating that Cr(VI) adsorption on Mam-F also obeyed the D–R isotherm. The values of q_{max} and K_{D-R} were obtained from the intercept and slope of the linear plots shown in the figures and were equal to 22.3 mg/g and -9×10^{-9} mol^2 kJ^{-2} at pH 6.5, with $R^2 = 0.9981$, and 87.4 mg/g and -1.0×10^{-9} mol^2 kJ^{-2} at pH 2.0, respectively, with $R^2 = 0.9909$. E, the mean free energy of the adsorption process, is defined as the free energy transferred for one mole of solute in solution. Using the equation $E = 1/\sqrt{-2K_{D-R}}$, the values of E were evaluated for both pH 6.5 and 2, and were equal to $E_{6.5} = 7,453.66$ kJ mol^{-1} and $E_{2.0} = 22,360.68$ kJ mol^{-1}. The high values of $E_{6.5}$ and $E_{2.0}$ indicated that the potential energy barrier for Cr(VI) adsorption on Mam-F was high.
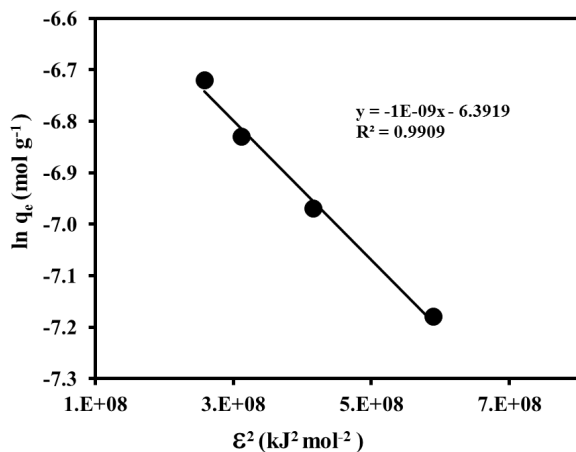
As just described the Cr(VI) adsorption data obtained when chromium concentration effect was searched fitted well to the three models (Freundlich, Langmuir and D–R) surveyed at the pH values of 2 and 6.5. According to the values of R^2 values, at pH 2 the order was $R^2_{Freundlich} > R^2_{Langmuir} > R^2_{D-R}$; while at pH 6.5 the order was $R^2_{D-R} > R^2_{Freundlich} > R^2_{Langmuir}$. As can be seen, for the two values of pH surveyed the best fitting was found for the D–R isotherm with $R^2 = 0.9981$ at pH 6.5. In relation to the parameter q_{max}, when comparing these values obtained from the application of Langmuir and D–R models, it can be observed that at pH 2 the q_{max} values were higher (64.87 and 87.24, respectively) than those obtained at pH 6.5 (9.48 and 22.3, respectively) for both models.

The maximum adsorption capacity (q_{max}) at pH 2 of Cr(VI) onto Mam-F, as obtained from Langmuir isotherm, was compared with the q_{max} values obtained at acidic pH values of several low-cost biosorbents reported in the literature (Table 1). As seen, Mam-F in this work possesses a high maximum adsorption capacity in comparison with some of the biosorbents displayed in Table 1.

3.4. Thermodynamics of the sorption processes

The results showed that the amount of Cr(VI) adsorbed at equilibrium increased with an increase in temperature. Using the temperature dependence data, the standard enthalpy, $\Delta H°$, standard entropy, $\Delta S°$, and Gibbs free energy, $\Delta G°$, were evaluated according to the following expressions (Eqs. (7) and (8)):

$$\ln K_c = -\frac{\Delta H°}{2.303RT} + \frac{\Delta S°}{2.303R} \tag{7}$$

$$\Delta G° = -RT\ln K_c \tag{8}$$

where $K_c = q_e/C_e$ [37]. The definitions of q_e and C_e are identical to those used in the adsorption isotherm section. T is the temperature in degrees Kelvin, and R is the gas constant (8.3143 kJ K^{-1} mol^{-1}). Using the linearized form of the van't

Fig. 9. Sorption isotherm of Cr(VI) by Mam-F at pH 2.0 fitted to the Dubinin–Radushkevich model.
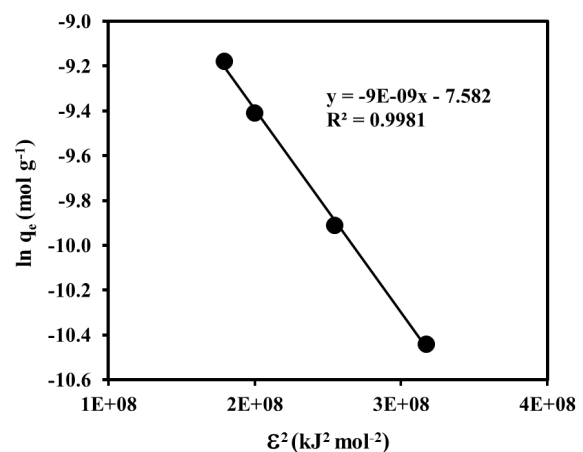
Fig. 10. Sorption isotherm of Cr(VI) by Mam-F at pH 6.5 fitted to the Dubinin–Radushkevich model.

Hoff equation (Eq. (7)), $\Delta H°$ and $\Delta S°$ were calculated from the slope and intercept of the straight line obtained when $\ln K_c$ was plotted vs. $1/T$ (Fig. 11). Table 2 displays the thermodynamic parameters of Cr(VI) adsorption onto Mam-F. The positive value of $\Delta H°$ (159.23 kJ mol^{-1}) indicated that the

Cr(VI) adsorption process was endothermic. Similarly, $\Delta S°$ was also positive (471.97 kJ K^{-1} mol^{-1}), which showed that the degrees of freedom increases due to adsorption. The Gibbs free energies, which were calculated using Eq. (8) at each temperature, are also given in the same table. The positive values of this thermodynamic parameter suggested that Cr(VI) adsorption onto Mam-F was not spontaneous.

Table 1
Maximum capacities of adsorbents obtained from biomasses for chromium removal

Adsorbent	q_{max} (mg/g)	pH	Reference
Potato peels	3.28	2.5	[5]
Formaldehyde-modified pomegranate peel	16.93[a]	3.0	[6]
Sargassum tunbergui Kunste	96.45	2.0	[7]
Chitosan-coated oxidized palm branches	55.0	6.0	[11]
Alligator weed	82.57	1.0	[9]
Fibers of *Ficus carica*	19.68	3.0	[12]
Mosambi fruit peelings	28.09	6.0	[14]
Activated carbon from tamarind wood	28.02	6.5	[18]
Biochar produced from rice husk and impregnated with Fe^{3+}	58.48	7.0	[32]
Agroforestry waste mixture	23.80	5.0	[33]
Amine-functionalized modified rice straw	21.87	2.0	[34]
Saccharomyces cerevisiae immobilized in glutaraldehyde cross-linked cellulose	23.61	2.5	[35]
Pleorotus streatus	10.75	2.5	[36]
Mammea americana	64.87	2.0	Present work

[a]Obtained by Dubinin–Radushkevich.

3.5. Characterization

3.5.1. SEM images

Figs. 12(a) and (b) display the SEM images of Mam-F before and after contact with the chromate solution at pH 2, respectively. As shown in the figure, the surface of the non-living biomass before Cr(VI) adsorption was highly corrugated due to the presence of thin walls and open cavities with diameters ranging from a few micrometers to 50 μm. After chromium adsorption, the Mam-F-Cr surface remained

Table 2
Thermodynamic parameters for the adsorption of Cr(VI) by Mam-F

Temperature (K)	Equilibrium constant, K_c	$\Delta G°$ (kJ/mol)
303	0.060	7,079.0
313	0.137	5,178.7
323	0.310	3,142.1
333	0.531	1,744.3
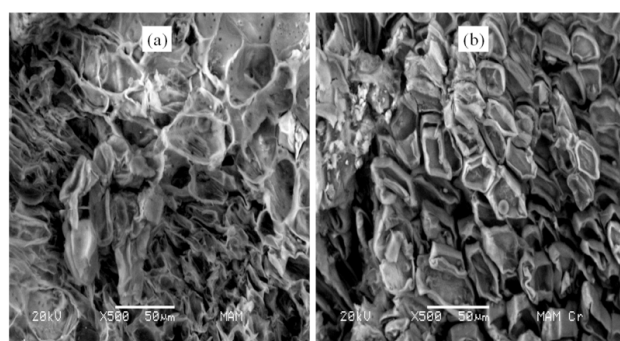
Fig. 12. SEM images of Mam-F before (a) and after (b) the contact with the Cr(VI) aqueous solution.

Fig. 11. LnK_c as a function of $1/T$ for the Cr(VI) adsorption by Mam-F.

$$y = -8.316x + 24.649$$
$$R^2 = 0.9853$$
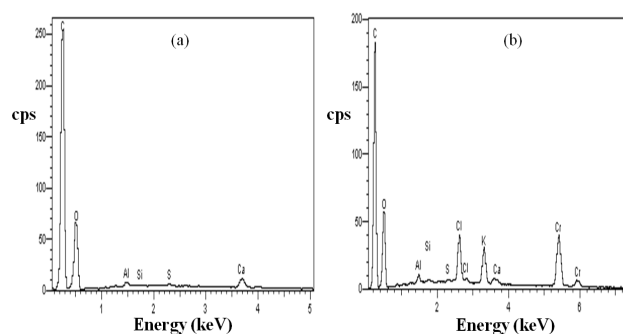
Fig. 13. Energy patterns of (a) Mam-F and (b) Mam-Cr(VI).
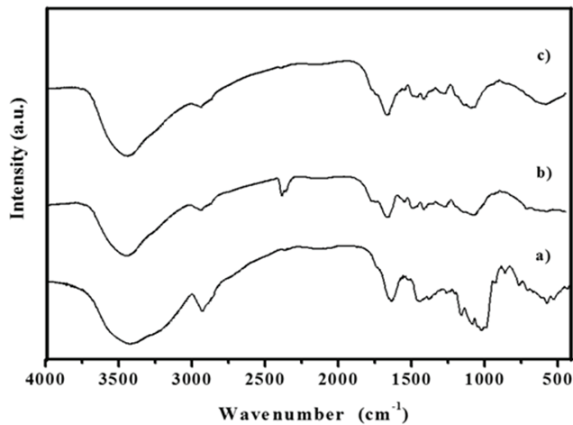
Fig. 14. FT-IR spectra of Mam (a), Mam-F (b) and Mam-F-Cr(VI) (c) samples.

Fig. 15. pH value of the point of zero charge for Mam-F.

corrugated, but the diameter of the cavities decreased (~25 μm) and the walls looked thicker.

3.5.2. Elemental analyses by energy dispersive X-ray spectroscopy (EDS)

The energy patterns of Mam-F before (Mam-F) and after (Mam-F-Cr(VI)) chromium adsorption are displayed in Figs. 13(a) and (b). The elemental composition of Mam-F was the following: C (55.38 ± 0.48 wt%), O (43.21 ± 0.68 wt%), Ca (1.04 ± 0.09 wt%), S (0.08 ± 0.007 wt%), Si (0.07 ± 0.007 wt%) and Al (0.20 ± 0.06 wt%). For Mam-F-Cr(VI), Cr was also detected, and the following elemental composition was obtained: C (50.19 ± 0.18 wt%), O (35.66 ± 0.06 wt%), Ca (0.25 ± 0.05 wt%), S (0.09 ± 0.01 wt%), Si (0.11 ± 0.008 wt%), Al (0.38 ± 0.009 wt%); Cl (2.79 ± 0.01 wt%), K (2.61 ± 0.01 wt%) and Cr (7.96 ± 0.04 wt%). Cl was derived from the HCl used to adjust the pH of the Cr(VI) solutions to 2, and the K content could be explained for the salt used to prepare the Cr(VI) solutions, which was K_2CrO_4.

3.5.3. FT-IR Spectroscopy

Fig. 14 shows the FT-IR spectra of Mam (a), Mam-F (b) and Mam-F-Cr(VI) (c). Characteristic peaks obtained for raw mamey husk are as follows: the band at 3,422.3 cm^{-1} was indicative of the existence of bonded hydroxyl groups, The peak at 2,927.5 cm^{-1} corresponded to asymmetric –CH$_2$ stretching; the 1,631.1 cm^{-1} band was attributed to CO stretching mode conjugated to the NH deformation mode, which suggested the presence of an amide; and the peak observed at 1,439.5 cm^{-1} was due to a bending of the O–H bond. The band at 1,159.2 cm^{-1} indicated a C–O stretching, while the peak at 1,082.4 cm^{-1} can be attributed to an alcoholic C–O group and the 1,045.8 cm^{-1} band can be a result of C–O stretching of alcoholic groups of polysaccharide. The main bands in the infrared spectrum of the biomaterial Mam-F were identified as follows: the peak at 3,439.5 cm^{-1} corresponded to –OH groups. The band at 2,924 cm^{-1} was attributed to asymmetric –CH$_2$ stretching. The trough at 1,736 cm^{-1} was indicative of an ester group. The 1,631.6 cm^{-1} band corresponded to the CO stretching mode, conjugated to the NH deformation mode, which suggested the presence of an amide (1,700–1,490 cm^{-1}).
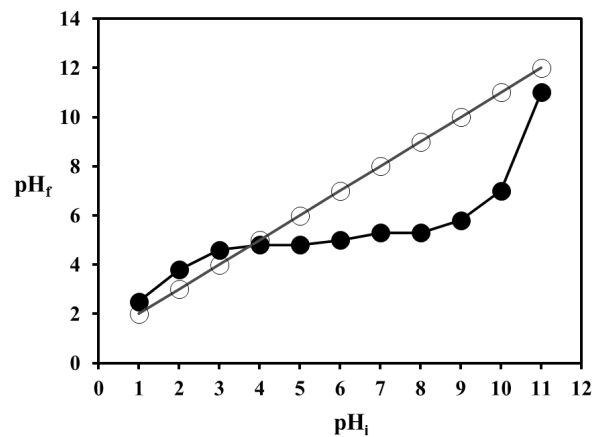
The bands observed at 1,140–930 cm^{-1} were assigned to C–O groups. After the Cr(VI) adsorption process was performed at pH 2, changes in the IR spectrum of Mam-F-Cr(VI) were not detected, except in the 1,000–400 cm^{-1} range, where small bands were observed at 733 and 871 cm^{-1}, which were assigned to CrO_4^{2-} present in the Mam-F-Cr(VI) sample.

3.5.4. pH of the point of zero charge (pH_{pzc})

The pH_{pzc} is the pH that corresponds to the net surface charge of the sorbent and indicates the preference of ionic species by the sorbent. According to the modified drift method, which was used to obtain the plot shown in Fig. 15, the pH of the pzc is determined by the intersect of the curve and a straight line with a slope equal to 1 [38]. Thus, the pzc for Mam-F was pH = 5.0. At pH values <5.0, the surface of Mam-F possessed a positive charge, allowing the non-living biomass (Mam-F) to adsorb anions. At pH values >5.0, the surface of Mam-F possessed a negative charge. Therefore, at pH 2, Mam-F adsorbed greater amounts of Cr(VI) in the form of $HCrO_4^-$ ions, while at pH 5.5, the adsorption of Cr(VI) in the form of $HCrO_4^-$ and CrO_4^{2-} ions notably diminished.

4. Conclusions

The pH of the chromate solution had a strong effect on the adsorption of chromium on mamey (*Mammea americana* L.) husks chemically modified by formaldehyde (Mam-F). Cr(VI) sorption was the highest at pH 2 and then decreased as the pH increased to alkaline values. The kinetics of chromate ion adsorption onto Mam-F indicated that equilibrium was achieved in ~20 h, and the experimental data fit the pseudo-second-order model. Cr(VI) adsorption was also affected by the initial chromium concentration and temperature. At pH 6.5 and 2, the Cr(VI) adsorption data for Mam-F fit the Freundlich, Langmuir and D–R isotherms, but the highest value of R^2 was obtained using the D–R model at pH 6.5. According to q_{max} of the Langmuir model, at 20°C, 7 times more Cr(VI) was adsorbed at pH 2 than at pH 6.5. The thermodynamic parameters showed that Cr(VI) adsorption by Mam-Fe was an endothermic, non-spontaneous process.

Acknowledgment

References

[1] H. Li, Z. Li, T. Liu, X. Xiao, Z. Peng, L. Deng, A novel technology for biosorption and recovery hexavalent chromium wastewater by biofunctional magnetic beds, Bioresour. Tehnnol., 99 (2008) 6271–6279.

[2] K.O. Olayinka, B.I. Alo, T. Adu, Sorption of heavy metals from electroplating effluents by low cost adsorbents II. Use of waste tea, coconut shell and coconut husk, J. Appl. Sci., 7 (2007) 2307–2313.

[3] U.K. Garg, M.P. Kaur, K. Garg, Removal of hexavalent chromium from aqueous solution by agricultural waste biomass, J. Hazard. Mater., 140 (2007) 60–68.

[4] V. Sarin, K.K. Pant, Removal of chromium from industrial waste by using eucalyptus bark, Bioresour. Technol., 97 (2006) 15–20.

[5] F. Mutongo, O. Kuipa, K.P. Kuipa, Removal of Cr(VI) from aqueous solutions using powder of potato peelings as a low cost sorbent, Bioinorg. Chem. Appl., 2014 (2014) 7.

[6] T.S. Najim, S.A. Yassin, Removal of Cr(VI) from aqueous solution using modified pomegranate peel: equilibrium and kinetic studies, E-J. Chem., 6 (2009) S129–S142.

[7] Y. Wang, Y. Li, F.J. Zhao, Biosorption of chromium(VI) from aqueous solutions by *Sargassum thunbergii* Kuntze, Biotechnol. Biotechnol. Equip., 28 (2014) 259–265.

[8] G. Moussavi, B. Barikbin, Biosortpion of Cr(VI) from industrial wastewater onto pistachio hull waste biomass, Chem. Eng. J., 162 (2010) 893–900.

[9] Z.S. Wang, Y.P. Tang, S.R. Tao, Removal of Cr(VI) from aqueous solutions by the nonliving biomass of Alligator weed: kinetics and equilibrium, Adsorption, 14 (2008) 823–830.

[10] E. Malkoc, Y. Nuhoglu, M. Dundar, Adsorption of chromium (VI) on pomace—an olive industrial waste: batch and column studies, J. Hazard. Mater., 138 (2006) 142–151.

[11] M.A. Shouman, N.A. Fathy, S.A. Khedr, A.A. Attia, Comparative biosorption studies of hexavalent chromium ion onto raw and modified palm branches, Adv. Phys. Chem., 2013 (2013) 9.

[12] V.K. Gupta, D. Pathania, S. Agarwal, S. Sharma, Removal of Cr(VI) onto *Ficus carica* biosorbent from water, Environ. Sci. Pollut. Res., 20 (2013) 2632–2644.

[13] G.S. Agarwal, H.K. Bhuptawat, S. Chaudhari, Biosorption of aqueous chromium(VI) by *Tamarindus indica* seeds, Bioresour. Tehnnol., 97 (2006) 949–956.

[14] R.H. Krishna, A.V.V.S. Swamy, Studies on removal of Cr(VI) from aqueous solutions using powder of Mosambi fruit peeling (PMFP) as a low cost sorbent, E-J. Chem., 9 (2012) 1389–1399.

[15] L. Levankumar, V. Muthukumaran, M.B. Gobinath, Batch adsorption and kinetics of Cr(VI) removal from aqueous solutions by *Ocimum americanum* L. seed pods, J. Hazard. Mater., 16 (2009) 709–713.

[16] R. Elangovan, L. Philip, K. Chandraraj, Biosorption of hexavalent and trivalent chromium by palm flower (*Borassus aethiopum*), Chem. Eng. J., 141 (2008) 99–111.

[17] V.B. Babu, S. Gupta, Adsorption of chromium using activated neem leaves as an adsorbent: kinetic studies, Adsorption, 14 (2008) 85–92.

[18] J. Acharya, J.N. Sahu, B.K. Sahoo, C.R. Mohanty, B.C. Meikap, Removal of chromium(VI) from wastewater by activated carbon from tamarind wood activated with zinc chloride, Chem. Eng. J., 150 (2009) 25–39.

[19] I. Acosta, P. Sandoval, D. Bautista, N. Hernández, J.F. Cárdenas, V.M. Martínez, Cr(VI) bioadsorption by the mamey husk (*Mammea americana L.*), Av. Cien. Ing., 3 (2012) 1–9.

[20] B.V. Babu, S. Gupta, Removal of Cr(VI) from wastewater using activated tamarind seeds as an adsorbent, J. Environ. Eng. Sci., 7 (2008) 553–557.

[21] P.C.C. Faria, J.J.M. Orfao, M.F.R. Pereira, Adsorption of anionic and cationic dyes on activated carbons with different surface chemistries, Water Res., 38 (2004) 2043–2052.

[22] M.A.A. Zaini, R. Okayama, M. Machida, Adsorption of aqueous metal ions on cattle-manure-compost based activated carbons, J. Hazard. Mater., 170 (2009) 1119–1124.

[23] W. Ma, N. Zhao, G. Yang, L. Tian, R. Wang, Removal of fluoride ions from aqueous solution by the calcination product of Mg-Al-Fe hydrotalcite-like compound, Desalination, 268 (2011) 20–26.

[24] I. Puigdomenech, Chemical Equilibrium Diagrams, MEDUSA Program, Inorganic Chemistry, Royal Institute of Technology, Stockholm, Sweden, 2004. Available from: http://www.inorg.Kth.se/Research/Ignasi;/index.html

[25] J.A. Solís-Fuentes, R.C. Ayala-Tirado, A.D. Fernández-Suárez, Mamey sapote seed soil (*Pouteria sapota*). Potential, composition, fractionation and thermal behavior, Grasas Aceites, 66 (2015) 1–10.

[26] I. Alia-Tejacal, R. Villanueva-Arce, C. Pelayo-Zaldívar, Postharvest physiology and technology of sapote mamey fruit (*Pouteria sapota* (Jacq.) H.E. Moore & Stearn), Postharvest Biol. Technol., 45 (2007) 285–297.

[27] B. Saha, C. Orvig, Biosorbents for hexavalent chromium elimination from industrial and municipal effluents, Coord. Chem. Rev., 254 (2010) 2959–2972.

[28] J. Wang, C. Chen, Biosorption of heavy metals by *Saccharomyces cerevisiae*: a review, Biotechnol. Adv., 24 (2006) 427–451.

[29] K.M. Al-Qahtani, Water purification using different waste fruit cortexes for the removal of heavy metals, J. Taibah Univ. Sci., 10 (2016) 700–708.

[30] Y.S. Ho, G. McKay, Pseudo-second-order model for sorption processes, Process Biochem., 34 (1999) 461–465.

[31] G. McKay, H.S. Blair, J.R. Garden, Adsorption of dyes on chitin. 1. Equilibrium studies, J. Appl. Polym. Sci., 27 (1982) 3043–3057.

[32] E. Agrafioti, D. Kalderis, E. Diamadopoulos, Ca and Fe modified biochars as adsorbents of arsenic and chromium in aqueous solutions, J. Environ. Manage., 146 (2014) 444–450.

[33] E. Rosales, L. Ferreira, M.A. Sanromán, T. Tavares, M. Pazos, Enhanced selective metal adsorption on optimised agroforestry waste mixtures, Bioresour. Technol., 182 (2015) 41–49.

[34] Y. Wu, Y. Fan, M. Zhang, Z. Ming, S. Yang, A. Arkin, P. Fang, Functionalized agricultural biomass as a low-cost adsorbent: utilization of rice straw incorporated with amine groups for the adsorption of Cr(VI) and Ni(II) from single and binary systems, Biochem. Eng. J., 105 (2016) 27–35.

[35] T. Sathvika, Manasi, V. Rajesh, N. Rajesh, Microwave assisted immobilization of yeast in cellulose biopolymer as a green adsorbent for the sequestration of chromium, Chem. Eng. J., 279 (2015) 38–46.

[36] A. Javaid, R. Bajwa, U. Shafique, J. Anwar, Removal of heavy metals by adsorption on *Pleurotus ostreatus*, Biomass Bioenergy, 35 (2011) 675–682.

[37] H. Ucun, K.Y. Bayhan, Y. Kaya, Kinetic and thermodynamic studies of the biosorption of Cr(VI) by *Pinus silvestry* Linn., J. Hazard. Mater., 153 (2008) 52–59.

[38] M.V. Lopez-Ramon, F. Stoeckli, C. Moreno-Castilla, F. Carrasco-Marín, On the characterization of acidic and basic surface sites on carbons by various techniques, Carbon, 37 (1999) 1215–1221.